ARTICLE

Conversion of Bio-syngas to Liquid Hydrocarbon over CuCoMn-Zeolite Bifunctional Catalysts

Zhao-xia Zhang, Pei-yan Bi, Pei-wen Jiang, Quan-xin Li*

Department of Chemical Physics, Anhui Province Key Laboratory of Biomass Clean Energy, University of Science and Technology of China, Hefei 230026, China

A series of bifunctional catalysts composed of a component for higher alcohol synthesis (Cu-CoMn oxides, CCM) and an acidic zeolite (SAPO-34, ZSM-5, Y, MCM-41) were prepared for production of liquid hydrocarbon directly from a bio-syngas through a one-stage process. The effects of zeolite type, zeolite content, Si/Al ratio and preparation method on catalyst texture and its reaction performance were investigated. Higher selectivities and yields of liquid products were obtained by using bifunctional catalysts. The yields of liquid hydrocarbons decreased in the order CCM-ZSM-5>CCM-SAPO-34>CCM-Y>CCM-MCM-41. CCM-ZSM-5 (20wt%, Si/Al=100) prepared by coprecipitation method displayed the optimal catalytic performance with the highest CO conversion (76%) and yield of liquid products (30%). The catalysts were characterized by N_2 adsorption/desorption, NH_3-TPD, XRD, and H_2-TPR analysis. The results showed that higher specific surface areas and pore volumes of bifunctional catalysts were achieved by adding zeolites into CuCoMn precursors. Medium pore dimension and moderate acidity in CCM-ZSM-5 were observed, which probably resulted in its excellent reaction performance. Additionally, a higher number of weaker acid sites (weak and/or medium acid sites) were formed by increasing ZSM-5 content in CCM-ZSM-5 or decreasing Si/Al ratio in ZSM-5. It was also seen that metal dispersion was higher and reducibility of metal ions was easier on the CCM-ZSM-5 catalyst prepared by coprecipitation. The higher alcohols-to-hydrocarbon process provides a promising route to hydrocarbon fuels via higher alcohols from syngas or biobased feedstocks.

Key words: Bifunctional, CuCoMn-zeolite, Higher alcohols-to-hydrocarbon process, Bio-syngas conversion, Liquid hydrocarbon synthesis

I. INTRODUCTION

With the gradual depletion of fossil fuel resources and environmental constraint, the production of clean fuels from syngas (CO and H_2) has attracted renewed attention [1−3]. Syngas is an important industrial feedstock which can be produced from coal, natural gas and biomass [4, 5]. Especially, as an abundant and renewable resource, biomass can contribute to a sustainable nonfossil-based raw material for energy sources or chemicals [6, 7]. Two major routes of liquid hydrocarbon production from syngas have been widely reported [8−12]. One was Fischer-Tropsch (FT) synthesis which was an important technology for conversion of syngas to liquid hydrocarbons and high value-added chemicals [9]. However, the FT process had two unfavorable disadvantages, namely nonselective product distribution controlled by Anderson-Schulz-Flory (ASF) polymerization kinetics and mainly linear hydrocarbons with

low octane value as gasoline [10]. The other route was methanol-to-gasoline (MTG) process which first converted syngas to methanol and then transformed methanol to hydrocarbons [11]. In recent decades, a number of researches have confirmed that the one-stage processes over bifunctional catalysts were more favourable for syngas conversion to gasoline than the two-stage and three-stage processes [9, 12]. With bifunctional catalyst, the synthesis of methanol from syngas on metallic sites and the transformation of methanol to hydrocarbons on acidic sites were allowed to occur simultaneously, which consequently thermodynamically enhanced methanol synthesis from syngas [9]. Moreover, the shape-selective properties of acidic function (*e.g.*, zeolites) limited the generation of large molecules. Therefore, bifunctional catalysts have been verified to show good performance companied with high conversion and product selectivity for syngas to liquid hydrocarbons in the MTG process.

Very recently, higher alcohols have also been reported to produce gasoline-range hydrocarbons, and showed higher yields of gasoline compared to methanol [13, 14]. Mentzel *et al.* [15] studied *i*-propanol which was used

─────────

*Author to whom correspondence should be addressed. E-mail: liqx@ustc.edu.cn, FAX: +86-551-63606689

as a reactant for conversion to gasoline over H-ZSM-5 zeolite. The results suggested that the total conversion capacity was more than 25 times higher for *i*-propanol than those for methanol and ethanol. Besides, the catalyst lifetime increased dramatically using *i*-propanol as the reactant. Thus, production of liquid hydrocarbons from syngas by the higher alcohols-to-hydrocarbon (HTH) route under MTG-like conditions has received great interest [9, 16]. Yan *et al.* have reported CuO-CoO-Cr$_2$O$_3$/H$^+$-ZSM-5 (C3Z) bifunctional catalysts prepared by physically mixing for CO hydrogenation to hydrocarbons [9]. Their results suggested that CO conversion and hydrocarbon yield increased when temperature and pressure increased. And hydrocarbon selectivity increased when H$_2$/CO ratio and space velocity of the feed gas decreased. Mohanty *et al.* have also synthesized (CuO-CoO-Cr$_2$O$_3$+MFI Zeolite) bifunctional catalysts for syngas conversion to liquid fuel [16]. Nevertheless, the HTH process for syngas to hydrocarbon via higher alcohols over bifunctional catalysts of higher alcohol synthesis catalyst and acidic zeolite has not been studied as extensively as that via methanol.

Several heterogeneous catalysts for higher alcohol synthesis from syngas have been explored and well reviewed [17]. Briefly, these catalysts can be classified into four types: (i) modified methanol synthesis catalysts [18, 19], (ii) modified Fischer-Tropsch synthesis catalysts [20−25], (iii) noble metals-based synthesis catalysts [26], and (iv) Mo-based synthesis catalysts [27, 28]. Among them, CuCo-based modified Fischer-Tropsch catalysts developed by Institut Francais du Petrole (IFP) have been regarded as one of the most promising catalysts for higher alcohol synthesis due to their relatively favorable reaction performance under mild operating conditions [9, 16]. In addition, migration of acid sites on different zeolites was also concerned for the bifunctional process [10]. Different zeolites (or more broadly molecular sieves) have clearly distinct properties in acidic nature and textural structure (*e.g.*, pore size, shape-selectivity) [29].

Our previous work mainly focused on bio-syngas production [30−32] and higher alcohol synthesis from bio-syngas over Na-promoted CuCoMn catalyst [33]. In this work, we study the influence of zeolite topology (SAPO-34, ZSM-5, Y, MCM-41) on the reaction performance of CuCoMn-zeolite bifunctional catalysts in producing liquid hydrocarbon directly from a bio-syngas. The selected zeolites possess small pore (SAPO-34, 0.43 nm), medium pore (ZSM-5, 0.54 nm×0.56 nm, 0.51 nm×0.54 nm), large pore (Y zeolite, 0.74 nm) of micropores and mesopore (MCM-41, 3.3 nm) respectively [34]. Furthermore, a comparision of two preparation methods for zeolite addition to CuCoMn precursor is conducted.

II. EXPERIMENTS

A. Catalyst preparation

Four types of zeolites (SAPO-34, ZSM-5, Y, MCM-41) supplied from Nankai University catalyst Co., Ltd. (Tianjin, China) were applied to prepare CuCoMn-zeolite bifunctional catalysts. ZSM-5 was pretreated by conversion of sodium form to protonated form [35]. The molar composition of the CuCoMn oxides was constant (Cu/Co/Mn=1/1/0.8) with a desired proportion of zeolite. The preparation process of CuCoMn-zeolite bifunctional catalysts is detailed as follows. A specific zeolite was blended with sodium carbonate (AR grade) solution (so-called co-precipitation method). Subsequently, the mixed solution of metal nitrate (AR grade) was quickly added into the alkali solution. The precipitate was aged in the mother liquor for 1 h, and then washed. After being dried at 393 K for 12 h, the solid was impregnated with appropriate amounts of Na$_2$CO$_3$ and kept at 343 K for 2 h, and then calcined in air at 723 K for 4 h. The obtained CuCoMn-zeolite sample was further pressed, crushed and sieved. The particles of 40−60 mesh were used for kinetic tests. Accordingly, the finally obtained CuCoMn-zeolite catalysts were designated as CCM-SAPO-34, CCM-ZSM-5, CCM-Y, and CCM-MCM-41, respectively. The catalyst without adding any zeolite was marked as CCM. In addition, for comparison of the influence of different preparation method on CuCoMn-zeolite bifunctional catalyst, ZSM-5 and calcinated CuCoMn oxieds were homogenized in a mortar (so-called physically mixing method). The mixture was then pelletized to tablets and broken into 40−60 mesh particles.

B. Catalyst characterization

Powder X-ray diffraction (XRD) patterns were recorded on an X'pert Pro Philips diffractometer (Philips, Netherlands), using a Cu Kα radiation (λ=0.15418 nm). The N$_2$ adsorption/desorption isotherms were performed at 77 K using the Micromeritics ASAP 2020 V3.00 analyzer. Brunauer-Emmett-Teller surface areas (S_{BET}) were evaluated from the linear part of the BET plots. Volumes (V) and average pore diameters (d) of mesopores were calculated using the Barrett-Joyner-Halenda (BJH) model on the desorption branch. The surface areas of micropores (S_{micro}) were measured by *t*-plot method. The volumes (V_{micro}) and median widths (d_{micro}) of micropores were determined by Horvath-Kawazoe method. H$_2$ temperature-programmed reduction (H$_2$-TPR) tests were carried out to study the reduction features of the catalysts in a home-built equipment. Prior to TPR experiments, the catalyst was treated in flowing Ar (30 mL/min) for 1 h. Subsequently, H$_2$ (5vol%, balance Ar) was switched on under argon flow (40 mL/min),

1. Shut off valve
2. Pressure indicator
3. Pressure controller
4. Mass flow controller
5. Micrometering valve
6. Furnace
7. Reactor
8. Temperature controller
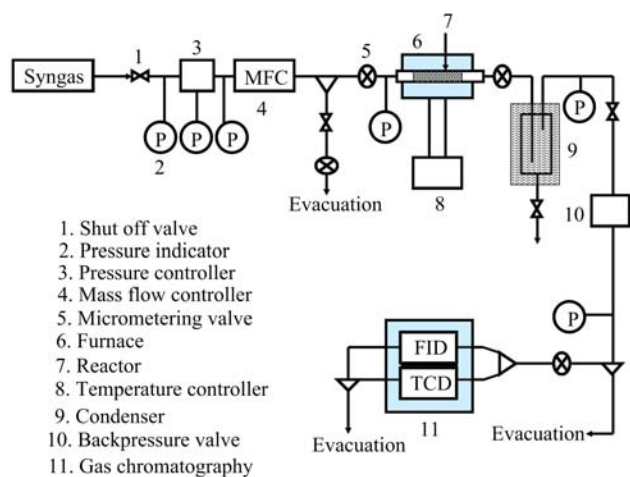9. Condenser
10. Backpressure valve
11. Gas chromatography

FIG. 1 Schematic setup of the fixed-bed flow reaction system for hydrocarbon synthesis from bio-syngas.

with the temperature increasing up to 973 K at a ramping rate of 10 K/min. The amount of hydrogen consumption was detected by a thermal conductivity detector (TCD) in an on-line gas chromatograph (GC). Ammonia temperature-programmed desorption (NH$_3$-TPD) experiments could provide the strengths and distributions of acid sites on catalysts. The NH$_3$-TPD tests were conducted following the procedure reported in Ref.[35].

C. Experimental setup and product analysis

The performance of hydrocarbon synthesis from bio-syngas was evaluated over bifunctional catalysts in a fixed-bed continuous-flow reactor system shown in Fig.1. The stainless steel (316 L) reactor was used with 10 mm internal diameter and 400 mm length. 1.0 g of the bifunctional catalyst along with inert material Pyrex beads was loaded in the reactor. Prior to catalytic evaluation experiments, the catalyst was activated *in situ* under H$_2$ flow (5vol%, balance Ar) at 523 K for 6 h. Thereafter, bio-syngas, including H$_2$, CO, CO$_2$, N$_2$, CH$_4$ and others with the volume contents of 62.80%, 30.89%, 2.96%, 1.75%, 1.20%, and 0.40%, respectively [33], was introduced into the reactor for hydrocarbon synthesis at the constant conditions: GHSV=4000 h^{-1}, T=563 K, and P=5 MPa with different bifunctional catalysts. Liquid products (aqueous and/or organic fractions) were cooled by ice from the gas and collected. The gaseous products were analyzed on-line by gas chromatograph (GC-SP6890). H$_2$, CO, CO$_2$, and CH$_4$ were measured by TDX-01 column with TCD detector. Gaseous hydrocarbons and aqueous fraction were determined by Porapak Q column with flame ionization detector (FID). The organic condensates were detected offline by SE30 capillary column with FID detector. The performance of hydrocarbon synthesis was evaluated by conversion of CO (C_{CO}), carbon selectivity of products (S_X), carbon yield of liquid products (Y_{liquid}) and carbon number distribution of liquid hydrocarbon products, according to the following equations:

$$C_{CO} = \frac{x_{inCO} - x_{outCO}}{x_{inCO}} \times 100\% \quad (1)$$

$$S_X = \frac{x_{certain}}{x_{inCO} - x_{outCO}} \times 100\% \quad (2)$$

$$Y_{liquid} = \frac{x_{liquid}}{x_{inCO}} \times 100\% \quad (3)$$

$$D = \frac{x_{hydro}}{x_{all}} \times 100\% \quad (4)$$

where x_{inCO} and x_{outCO} are moles of CO in and out; $x_{certain}$, x_{liquid}, x_{hydro}, and x_{all} are moles of carbon in a certain product, liquid products, C$_n$ hydrocarbon product or a fraction, and all liquid hydrocarbon products, respectively. The content of coke formed on the catalysts was negligent.

III. RESULTS AND DISCUSSION

A. Performance of liquid hydrocarbon synthesis

1. Effect of different zeolites

Bifunctional catalysts of CuCoMn oxides by coprecipitation of 20% (weight, similarly hereinafter) different zeolites (SAPO-34, ZSM-5, Y, MCM-41) for hydrocarbon synthesis were investigated under the constant conditions: GHSV=4000 h^{-1}, T=563 K, and P=5 MPa (the reaction conditions below unless specifically stated otherwise are the same as those described here), the results are shown in Fig.2. From Fig.2(a), CO conversions increased from 35% to 49%, 76%, and 45% when SAPO-34, ZSM-5, MCM-41 were introduced into CuCoMn oxides except for Y zeolite (34%). The selectivities toward liquid products (S_{liquid}, mainly including hydrocarbon and/or alcohols) increased over all CuCoMn-zeolite bifunctional catalysts with just a little increment from 28% to 29% over CCM-MCM-41. Y_{liquid}, a parameter combined with CO conversion and selectivity of liquid products, increased from 10% on CuCoMn oxides to 18%, 30%, 14%, and 13% corresponding to CCM-SAPO-34, CCM-ZSM-5, CCM-Y, and CCM-MCM-41, respectively. CCM-ZSM-5 showed the optimal catalytic activity and yield of desired products. With regard to the by-products, CO$_2$ was the primary product over zeolite-free CuCoMn catalyst and remarkably decreased over zeolite-containing bifunctional catalysts. By contrast, the selectivities of methane and C2-C4 gaseous hydrocarbons were enhanced with the addition of the zeolites.

Figure 2(b) shows the changes of liquid hydrocarbon distribution over CuCoMn-based bifunctional catalysts with different zeolites. The contents of products decreased as their carbon numbers increased over the
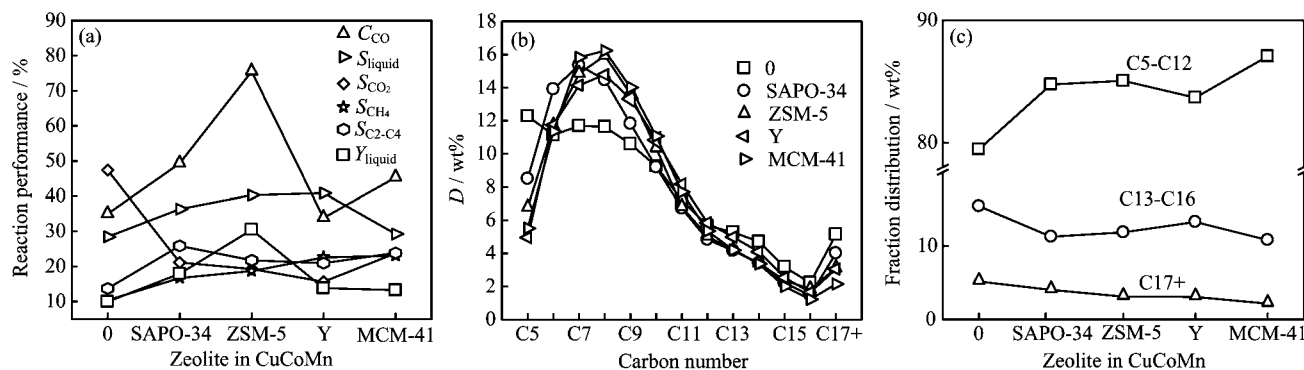
FIG. 2 The results of hydrocarbon synthesis reactions over bifunctional catalysts with CuCoMn oxide and 20wt% different zeolites prepared by coprecipitation. (a) Conversion of CO (C_{CO}), carbon selectivity of products (S_X) and carbon yield of liquid products (Y_{liquid}). (b) The carbon number distribution of hydrocarbon products. (c) The fraction distribution of hydrocarbon products. 0, means the CuCoMn oxide without adding zeolite; C17+, suggests the total content of C17 and larger than C17. The constant conditions: GHSV=4000 h^{-1}, T=563 K, P=5 MPa. The reaction conditions unless specifically stated otherwise are the same as those described here.
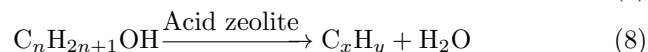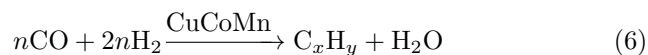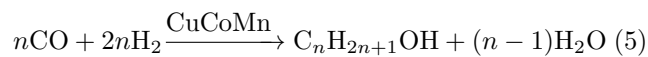
zeolite-free CuCoMn catalysts, which followed excellent Anderson-Schulz-Flory (ASF) ditributions except for a little deviation of ethanol from the ASF plots. On the other hand, the carbon numbers of hydrocarbons produced from CuCoMn-zeolites bifunctional catalysts were concentrated in the range of C6 to C10.

Figure 2(c) shows the fraction distribution of hydrocarbon more clearly. As shown in Fig.2(c), the C5-C12 fraction (a typical gasoline range product) increased and the heavier fractions (C13-C16, and C17+) decreased when zeolites were added into the CuCoMn oxides.

It should be particularly pointed out that zeolite-free CuCoMn catalyst is generally used for production of higher alcohols. Therefore, the liquid hydrocarbons shown in Fig.2 (b) and (c) were regarded as by-products and a few of them were formed with the selectivity of less than 10%.

The results indicate that bifunctional catalysts by introducing zeolites into CuCoMn-based higher alcohol synthesis catalyst enhance the reaction performance of syngas to hydrocarbon. By addition of zeolites, the increase of light fraction in liquid products implies that the cracking reactions of long-chain compounds are favored, which agrees with the increase in C1-C4 hydrocarbons.

The main reactions of syngas conversion on CuCoMn-zeolites bifunctional catalysts occur briefly as follows:

$$n\text{CO} + 2n\text{H}_2 \xrightarrow{\text{CuCoMn}} \text{C}_n\text{H}_{2n+1}\text{OH} + (n-1)\text{H}_2\text{O} \quad (5)$$

$$n\text{CO} + 2n\text{H}_2 \xrightarrow{\text{CuCoMn}} \text{C}_x\text{H}_y + \text{H}_2\text{O} \quad (6)$$

$$\text{CO} + \text{H}_2\text{O} \rightarrow \text{CO}_2 + \text{H}_2 \quad (7)$$

$$\text{C}_n\text{H}_{2n+1}\text{OH} \xrightarrow{\text{Acid zeolite}} \text{C}_x\text{H}_y + \text{H}_2\text{O} \quad (8)$$

Higher alcohols ($\text{C}_n\text{H}_{2n+1}\text{OH}$, $n \geq 2$) are synthesized from syngas on CuCoMn oxides (reaction (5)). Cop-

per sites are responsible for CO associative and hydrogen dissociative adsorption, while cobalt sites are responsible for CO dissociative adsorption, carbon chain growth, and hydrogenation [9]. Mn is an efficient promoter for increasing the production of ethanol [17]. At the same time, hydrocarbons (C_xH_y, mainly C1-C4 gaseous hydrocarbons) and CO_2 are formed as by-products (reactions (6) and (7)). The CO_2 selectivity amounted to ca. 47% over zeolite-free CuCoMn catalyst, indicating a relatively high activity for the water-gas-shift (WGS) reaction (reaction (7)). The addition of zeolites enables higher alcohols to convert into hydrocarbons on zeolite acid sites (reaction (8)) through alcohol dehydration to olefins [14], and in turn olefin oligomerization, aromatization, isomerization, cracking, hydrogen transfer, *etc*. The reacton (8) thermodynamically facilitates the reaction (5) to form higher alcohols from syngas and simultaneously suppresses the formation of by-products from side reactions (reaction (6) and (7)). Therefore, CO conversion and hydrocarbon selectivity increased while CO_2 selectivity decreased, as previously explained.

2. Effect of ZSM-5 content

Figure 3 shows the influence of different ZSM-5 contents (20% and 50%) on hydrocarbon synthesis over CuCoMn-ZSM-5 bifunctional catalysts prepared by coprecipitation method. When the content of ZSM-5 in bifunctional catalyst increased from 20% to 50%, CO conversion decreased from 76% to 51% while the changes of product selectivities were not obvious. This can be explained that much more metal active sites are covered by zeolite accompanying with the decrease in the metal number when ZSM-5 content increased. Thus, the yield of liquid products was higher on CuCoMn-ZSM-5 (20%) catalyst due to its higher CO conversion. From Fig.3(b), the carbon numbers
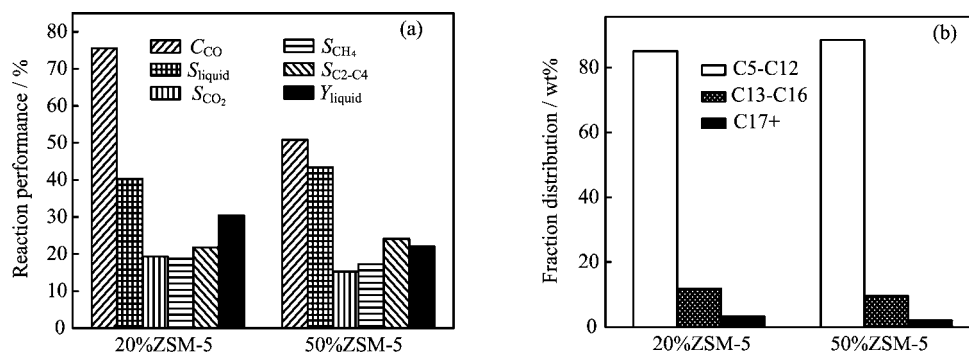
FIG. 3 The reaction results over bifunctional catalysts of CuCoMn oxide and ZSM-5 with different zeolite content.
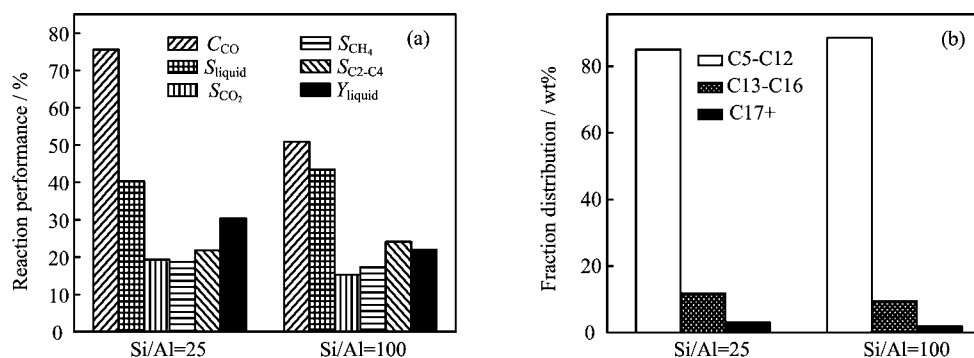

FIG. 4 The reaction results over bifunctional catalysts of CuCoMn oxide and ZSM-5 with different Si/Al ratio.

were mainly concentrated in the range of C5 to C12. The C5-C12 fraction increased from 85% to 89% and accordingly the heavier fractions (C13-C16, and C17+) decreased on CuCoMn-ZSM-5 (50%) catalyst. The results indicate that cracking reactions are more favorable to occur but the changes fluctuate within a narrow range with the increment of ZSM-5 content.

3. Effect of Si/Al ratio of ZSM-5

The Si/Al ratio of ZSM-5 used above was 100 and the ZSM-5 (Si/Al ratio 25) was employed for comparison. Figure 4 shows the effect of different Si/Al ratio of ZSM-5 on hydrocarbon synthesis over CuCoMn-ZSM-5 (20%) bifunctional catalysts prepared by coprecipitation method. CO conversions were 53% and 76% corresponding to the ZSM-5 with Si/Al ratio of 25 and 100 respectively. The selectivity of liquid product was higher on ZSM-5 (Si/Al=100) than that on ZSM-5 (Si/Al=25), and thereby with significantly higher yield. On the other hand, CO_2 selectivity was obviously lower on ZSM-5 (Si/Al=100) than that on ZSM-5 (Si/Al=25) and C1-C4 hydrocarbons were slightly higher correspondingly. Moreover, the fraction distributions were similar to each other. Combined with the reaction performance on zeolite-free CuCoMn catalyst, it is concluded that the improvement by adding ZSM-5 (Si/Al=25) to CuCoMn is not adequate, which

can be ascribed to the acidic nature owing to the Si/Al ratio (detailed discussions will be given below in NH_3-TPD analysis).

4. Effect of catalyst preparation method

Figure 5 shows the influence of different preparation methods of CuCoMn-ZSM-5 (20wt%, Si/Al=100) bifunctional catalysts on hydrocarbon synthesis. CO conversion, selectivity, and yield of liquid products were 49%, 30%, and 15% respectively by physically mixing method, all of which were lower than those by coprecipitation method. The selectivity of C1-C4 hydrocarbons followed similar trends. Oppositely, 42% of CO_2 selectivity corresponding to physically mixing method was much higher than that corresponding to coprecipitation method. The light fraction (C5-C12) was slightly lower and thereby with higher heavier fractions (C13-C16, and C17+) by physically mixing method. The results show that coprecipitation method is more favorable to prepare CuCoMn-ZSM-5 bifunctional catalysts.

Based on the results above, hybrid CuCoMn-ZSM-5 (20wt%, Si/Al=100) prepared by coprecipitation method is the optimal bifunctional catalyst having the ideal reaction performance for hydrocarbon synthesis from bio-syngas.
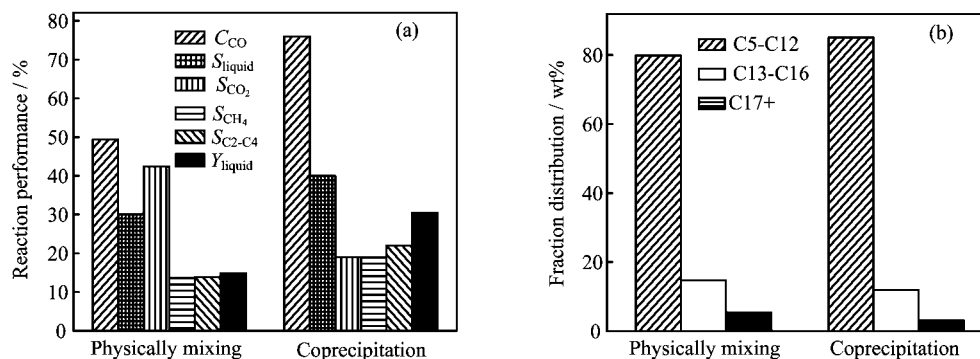

FIG. 5 The reaction results over bifunctional catalysts of CuCoMn oxide and ZSM-5 by different preparation method.

TABLE I Textural parameters of CuCoMn-zeolite catalysts.

Sample	$S_{BET}/(m^2/g)$	$V/(cm^3/g)$	d/nm	$S_{micro}/(m^2/g)$	$V_{micro}/(m^3/g)$	d_{micro}/nm
CCM	75	0.23	12.8	9	0.021	0.96
CCM-SAPO-34	94	0.31	9.5	17	0.029	0.60
CCM-ZSM-5[a]	117	0.25	8.4	39	0.041	0.50, 0.52[c]
CCM-Y	139	0.30	9.8	58	0.050	0.60
CCM-MCM-41	173	0.27	3.0, 7.4[b]	9	0.042	0.64
Pure ZSM-5	233	0.22	5.8	80	0.106	0.54, 0.56[c]
CCM+ZSM-5[b]	107	0.23		23	0.038	

[a] CCM-ZSM-5 was prepared by coprecipitation method with 20%ZSM-5 and Si/Al ratio of 100.
[b] There are two obvious peaks.
[c] The calculated value is the simple sum of 80%CuCoMn oxide and 20%ZSM-5 (Si/Al=100).

B. Characterization of catalysts

1. Textural and acid properties of CuCoMn-zeolite bifunctional catalysts

Textural properties were obtained from N_2 adsorption/desorption analysis. Table I lists the surface areas, pore volumes, and average pore diameters d of CuCoMn oxide, pure ZSM-5, and bifunctional catalysts with different zeolites (SAPO-34, ZSM-5, Y, MCM-41). When zeolites were added into CuCoMn precursor, S_{BET}, V, S_{micro} and V_{micro} of obtained bifunctional catalysts all increased except for S_{micro} of MCM-41 as MCM-41 is a mesoporous material with minute quantities of micropores. These rusults can be explained that zeolites are porous materials with large surface areas and volumes. With respect to the average diameters, pore sizes of bifunctional catalysts in the mesopore range were smaller than that of CuCoMn catalyst which is expected that added zeolites occupy part of channels. d of 3.0 nm in CCM-MCM-41 catalyst was identified as the long-range ordered mesopores from MCM-41. On the other hand, d_{micro} exhibited interesting tendencies. d_{micro} of CCM-ZSM-5 and CCM-Y catalysts were smaller than those of ZSM-5 and Y zeolites, which are attributed to the occupation of metal oxides. However, d_{micro} of 0.60 nm in CCM-SAPO-34 catalyst was larger than that of 0.43 nm in SAPO-34 zeolite. This

can be inferred that the micropores are formed mainly from metal oxides and metal oxides may block access to the micropores of SAPO-34 zeolite. The similar result was presumed in CCM-MCM-41 catalyst because mesoporous MCM-41 possesses small amount of micropore. These results shown above suggest that pore dimensions of the bifuntional catalysts are determined by the interaction of metal oxides and zeolites. In addition, the calculated values of (CCM+ZSM-5) by simply summing 80%CuCoMn oxide and 20%ZSM-5 were lower than those of CCM-ZSM-5 bifunctional catalyst prepared by coprecipitation, implying that incremental improvements in textural properties are achieved during the preparation process.

The surface acid properties of zeolite-containing samples were investigated by NH_3-TPD. The density of total acid sites and their distribution derived from NH_3-TPD profiles are summarized in Table II. The acid density of bifunctional catalysts containing 20% different zeolites decreased in the order CCM-Y>CCM-SAPO-34>CCM-ZSM-5 (Si/Al=100)>CCM-MCM-41, which did not follow the trends of liquid product yields (Fig.2(a), CCM-ZSM-5>CCM-SAPO-34>CCM-Y>CCM-MCM-41). The relatively low yield obtained from CCM-Y is particularly surprising, because CCM-Y had the highest density of acid sites. With respect to the strength

TABLE II Surface acidity and acid strength distribution on the catalysts[a].

Sample	Zeolite/%	Si/Al	Total acidity/ (μmol/g catalyst)	Percentage of acid sites[b]/%		
				Weak acid	Medium acid	Strong acid
CCM-SAPO-34	20		93	56.32	36.74	6.94
CCM-ZSM-5	20	100	75	55.50	39.35	5.15
CCM-Y	20		244	38.48	45.03	16.49
CCM-MCM-41	20		36	93.25	0.96	5.78
CCM-ZSM-5	50	100	185	75.73	22.39	1.88
CCM-ZSM-5	20	25	165	92.73	7.27	0.00
ZSM-5	100	25	590	25.93	30.28	43.79

[a] The acid density and distribution were estimated by the Gaussian fitting of NH_3-TPD profiles.
[b] Weak acid at 373−503 K, medium acid at 503−643 K, strong acid at 643−823 K.

of acid sites, CCM-SAPO-34 and CCM-ZSM-5 had similar distributions, in other words, they had around 55%−56% weak acid sites, 36%−40% medium acid sites and 5%−7% strong acid sites. CCM-MCM-41 had fewer total acid sites, and contained mainly weak acid sites with a small amount of medium and strong acid sites (less than 10%). By contrast, CCM-Y contained much more medium and strong acid sites than the others.

By linking the results of hydrocarbon synthesis over these bifunctional catalysts with their textural and surface acid properties, it can be concluded that excellent reaction performance CCM-ZSM-5 displays is correlated with the medium micropore and moderate acidity of ZSM-5. SAPO-34 with small pore apertures (0.43 nm) is suitable for production of light olefins such as ethene and propene [36]. Y zeolite with large micropore favors the formation of (poly)aromatic-type coke which hinders the reactants from accessing the active sites. In addition, excessive medium and strong acid sites may be another reason in favor of coke deposition and thereby lower activity [37, 38]. MCM-41 containing only a few weak acid sites leads to the acidic function of bifunctional catalyst unconspicuous. In contrast, the medium-pore ZSM-5 produces low amounts of (poly)aromatic-type coke as coke precursors are hindered inside the relatively narrow channels, thus retaining a larger number of acid sites for further reactions of the primary long-chain n-paraffins such as isomerization and cracking [37].

Therefore, ZSM-5 having moderate acidic properties and an MFI pore topology with an intersecting 10-membered ring pore system composed of straight (0.54 nm×0.56 nm) and sinusoidal (0.51 nm×0.54 nm) channels is suitable to constitute the CuCoMn-zeolite bifunctional catalyst for production of gasoline-range hydrocarbons directly from syngas [34, 36].

2. Acid properties of CuCoMn-ZSM-5 with different contents and Si/Al ratios of ZSM-5

The acid densities and distributions of CCM-ZSM-5 (Si/Al=100) with 20% and 50% ZSM-5 are listed in

Table II. CCM-ZSM-5 (50%) with a higher content of ZSM-5 contained about 2.5 times the number of acid sites than CCM-ZSM-5 (20%), in agreement with the increment of ZSM-5. However, the distributions of acid strength followed different trends. The percentage of weak acid sites in CCM-ZSM-5 (50%) catalyst increased while those of medium and strong acid sites decreased. Moreover, the absolute amounts of weak and medium acid sites increased compared to CCM-ZSM-5 (20%) catalyst, thus resulting in a slightly higher number of lighter compounds (C5-C12). From the NH_3-TPD analysis and the reaction performance discussed above, it is seen that increasing ZSM-5 content in the CCM-ZSM-5 leads to the increment of weak acid sites at the expense of catalytic activity due to the loss of metal active sites.

The acid properties of CCM-ZSM-5 (20%) with Si/Al=25 are also listed in Table II. CCM-ZSM-5 (Si/Al=25) with a lower framework Si/Al ratio contained more than twice the amount of acid sites than CCM-ZSM-5 (Si/Al=100). The weak acid sites increased from 55.50% to 92.73%. Surprisingly, strong acid sites disappeared. Compared with pure ZSM-5, the medium and strong acid sites in CCM-ZSM-5 (Si/Al=25) catalyst dramatically decreased. This result indicates that stronger acid sites preferentially interact with metal precursors, as also seen in CCM-ZSM-5 (50%, Si/Al=100) catalyst. Further inference can be made that the strong interaction of metal with acid sites of zeolite may weaken the interaction of metal with reactants. On the other hand, despite a higher density of acid sites in CCM-ZSM-5 (Si/Al=25), CO conversion and selectivity of liquid products were lower than those on CCM-ZSM-5 (Si/Al=100). This may result from the fact that weak acid sites are catalytically inactive for alcohols-to-hydrocarbon reactions as the case of CCM-MCM-41 [36].

3. Crystalline phases and reducibility on CCM-ZSM-5 prepared by different methods

The crystalline phases of samples were identified using XRD analysis. Figure 6(A) shows the XRD pat-
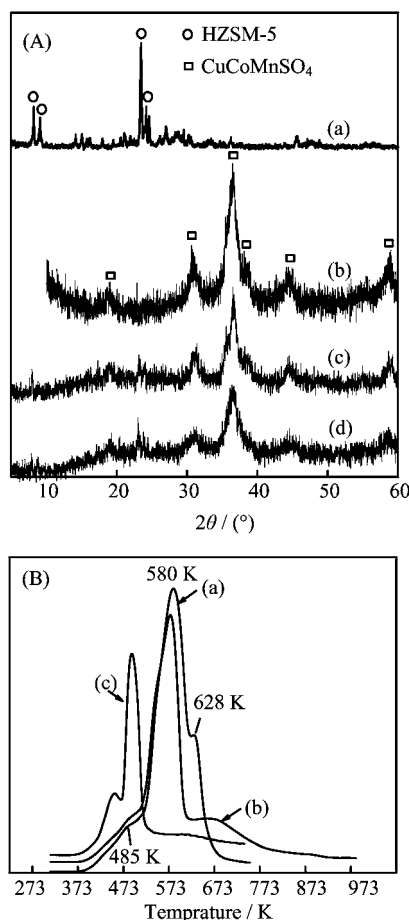
FIG. 6 The effect of preparation method on the properties of catalysts. (A) XRD patterns of (a) ZSM-5, (b) CuCoMn oxide, (c) CCM-ZSM-5 prepared by physically mixing, and (d) CCM-ZSM-5 prepared by coprecipitation, HZSM-5 (JCPDS 80-0922), CuCoMnO$_4$ (JCPDS 47-0324). (B) H$_2$-TPR profiles of (a) CuCoMn oxide, (b) CCM-ZSM-5 prepared by physically mixing, and (c) CCM-ZSM-5 prepared by coprecipitation.

terns of CCM-ZSM-5 catalysts prepared by physically mixing and coprecipitation methods. Compared with the diffraction peaks of pure ZSM-5 and CuCoMn oxide, the coexistence of HZSM-5 (JCPDS 80-0922) and spinel CuCoMnO$_4$ (JCPDS 47-0324) is presented in these two bifunctional catalysts. However, the XRD line width for the catalyst prepared by coprecipitation is broader. The average crystallite sizes of CuCoMnO$_4$ calculated by XRD line widths using Scherrer equation are 4.57 and 3.74 nm corresponding to physically mixing and coprecipitation methods. XRD results imply that metal dispersion is higher by coprecipitation and thereby with more favorable exposure of active sites on the surface.

The reducibility of samples was studied by H$_2$-TPR. Figure 6(B) illustrates the TPR profiles of CuCoMn oxide and CCM-ZSM-5 catalysts prepared by physically mixing and coprecipitation methods. Three peaks centered at 485, 580, and 628 K were observed for Cu-

CoMn oxide. The H$_2$ consumption peaks were assigned to the reduction of copper and manganese ions [9]. A slight shift in hydrogen consumption peaks towards lower temperature regions was observed for CCM-ZSM-5 prepared by physically mixing, and an obvious shift occurred for CCM-ZSM-5 prepared by coprecipitation. These shifts are in line with the XRD results that the reduction of metal ions is easier due to higher dispersion of metal precursors.

IV. CONCLUSION

A series of bifunctional catalysts comprising a higher alcohol-synthesis component (CuCoMn oxides) and an acidic zeolite (SAPO-34, ZSM-5, Y, MCM-41) were successfully applied to enhance both the selectivity and yield of liquid hydrocarbon produced directly from a bio-syngas. The liquid product yields decreased in the order CCM-ZSM-5>CCM-SAPO-34>CCM-Y>CCM-MCM-41. The enhancement of reaction performance by using bifunctional catalysts can be attributed to the displacement of thermodynamic equilibrium of higher alcohol synthesis and the textural improvements (*e.g.*, the increments of surface area and volume). ZSM-5 zeolite was preferred to be used as the acidic function in CuCoMn-zeolite bifunctional catalysts owing to its highest CO conversion (76%) and carbon yield of liquid product (30%) among four selected zeolites. The excellent reaction performance CCM-ZSM-5 exhibits is correlated with the moderate acidic properties and medium micropore of ZSM-5 with a particular topology. In addition, increasing ZSM-5 content in the CCM-ZSM-5 led to the increment of weak and medium acid sites at the expense of catalytic activity due to the loss of metal active sites. Decreasing Si/Al ratio in ZSM-5 induced the increase of weak acid sites and decrease of medium and strong acid sites. Accordingly, the CCM-ZSM-5 (Si/Al=25) with a lower Si/Al ratio showed lower CO conversion and product selectivity. Moreover, the CCM-ZSM-5 catalyst prepared by coprecipitation displayed higher metal dispersion and easier reducibility of metal ions. In the present study, the optimal bifunctional catalyst of CuCoMn-ZSM-5 (20wt%, Si/Al=100) prepared by coprecipitation method was obtained for transformation of bio-syngas into liquid hydrocarbon.

V. ACKNOWLEDGMENTS

[1] M. R. Morrill, N. T. Thao, H. Shou, R. J. Davis, D. G. Barton, D. Ferrari, P. K. Agrawal, and C. W. Jones,

ACS Catal. **3**, 1665 (2013).

[2] L. Zhou, H. Yang, H. Wu, M. Wang, and D. Cheng, Fuel Process Technol. **106**, 385 (2013).

[3] K. Atsonios, C. Christodoulou, E. I. Koytsoumpa, K.D. Panopoulos, and E. Kakaras, Biomass Bioenerg. **53**, 54 (2013).

[4] V. P. Santos, B. van der Linden, A. Chojecki, G. Budroni, S. Corthals, H. Shibata, G. R. Meima, F. Kapteijn, M. Makkee, and J. Gascon, ACS Catal. **3**, 1634 (2013).

[5] Q. Xie, S. Kong, Y. Liu, and H. Zeng, Bioresour. Technol. **110**, 603 (2012).

[6] R. M. Navarro, M. A. Pena, and J. L. G. Fierro, Chem. Rev. **107**, 3952 (2007).

[7] R. D. Cortright, R. R. Davda, and J. A. Dumesic, Nature **418**, 964 (2002).

[8] A. V. Bridgwater and G. V. C. Peacocke, Renew. Sust. Energ. Rev. **4**, 1 (2000).

[9] Q. Yan, P. T. Doan, T. Hossein, C. G. Amit, and G. W. Mark, J. Phys. Chem. C **112**, 11847 (2008).

[10] F. G. Botes and W. Böhringer, Appl. Catal. A **267**, 217 (2004).

[11] R. A. Comelli and N. S. Fgoli, Ind. Eng. Chem. Res. **32**, 2414 (1993).

[12] V. M. Mysov, S. I. Reshetnikov, V. G. Stepanov, and K. G. Ione, Chem. Eng. J. **107**, 63 (2005).

[13] N. R. C. F. Machado, V. Calsavara, N. G. C. Astrath, C. K. Matsuda, A. P. Junior, and M. L. Baesso, Fuel **84**, 2064 (2005).

[14] A. C. Gujar, V. K. Guda, M. Nolan, Q. Yan, H. Toghiani, and M. G. White, Appl. Catal. A **363**, 115 (2009).

[15] U. V. Mentzel, S. Shunmugavel, S. L. Hruby, C. H. Christensen, and M. S. Holm, J. Am. Chem. Soc. **131**, 17009 (2009).

[16] P. Mohanty, K. K. Pant, J. Parikh, and D. K. Sharma, Fuel Process. Technol. **92**, 600 (2011).

[17] V. Subramani and S. K. Gangwal, Energ. Fuel. **22**, 814 (2008).

[18] E. Heracleousa, E. T. Liakakoua, A. A. Lappas, and A. A. Lemonidou, Appl. Catal. A **455**, 145 (2013).

[19] R. G. Herman, Catal. Today **55**, 233 (2000).

[20] V. Mahdavi and M. H. Peyrovi, Catal. Commun. **7**, 542 (2006).

[21] N. Tien-Thao, M. H. Zahedi-Niaki, H. Alamdari, and S. Kaliaguine, J. Catal. **245**, 348 (2007).

[22] R. Xu, W. Wei, W. H. Li, T. D. Hu, and Y. H. Sun, J. Mol. Catal. A **234**, 75 (2005).

[23] R. Xu, C. Yang, W. Wei, W. H. Li, Y. H. Sun, and T. D. Hu, J. Mol. Catal. A **221**, 51 (2004).

[24] H. B. Zhang, X. L. Liang, X. Dong, H. Y. Li, and G. D. Lin, Catal. Surv. Asia **13**, 41 (2009).

[25] X. Dong, X. L. Liang, H. Y. Li, G. D. Lin, P. Zhang, and H. B. Zhang, Catal. Today **147**, 158 (2009).

[26] M. Ojeda, M. L. Granados, S. Rojas, P. Terreros, F. J. Garcia-Garcia, and J. L. G. Fierro, Appl. Catal. A **261**, 47 (2004).

[27] J. Iranmahboob, H. Toghiani, D. O. Hill, and F. Nadim, Fuel Process. Technol. **79**, 71 (2002).

[28] Z. Li, Y. Fu, J. Bao, M. Jiang, T. Hu, T. Liu, and Y. N. Xie, Appl. Catal. A **220**, 21 (2001).

[29] E. Taarning, C. M. Osmundsen, X. Yang, B. Voss, S. I. Andersen, and C. H. Christensen, Energy Environ. Sci. **4**, 793 (2011).

[30] T. Kan, J. X. Xiong, X. L. Li, T. Q. Ye, L. X. Yuan, Y. Torimoto, M. Yamamoto, and Q. X. Li, Int. J. Hydrogen Energy **35**, 518 (2010).

[31] L. X. Yuan, Y. Q. Chen, C. F. Song, T. Q. Ye, Q. X. Guo, Q. S. Zhu, Y. Torimoto, and Q. X. Li, Chem. Commun. **7**, 5215 (2008).

[32] T. Q. Ye, L. X. Yuan, Y. Q. Chen, T. Kan, J. Tu, X. F. Zhu, Y. Torimoto, M. Yamamoto, and Q. X. Li, Catal. Lett. **127**, 323 (2009).

[33] T. Q. Ye, Z. X. Zhang, Y. Xu, S. Z. Yan, J. F. Zhu, Y. Liu, and Q. X. Li, Acta Phys. Chim. Sin. **27**, 1493 (2011).

[34] J. Jae, G. A. Tompsett, A. J. Foster, K. D. Hammond, S. M. Auerbach, R. F. Lobo, and G. W. Huber, J. Catal. **279**, 257 (2011).

[35] F. Gong, Z. Yang, C. Hong, W. Huang, S. Ning, Z. Zhang, Y. Xu, and Q. Li, Bioresour. Technol. **102**, 9247 (2011).

[36] J. Kim, M. Choi, and R. Ryoo, J. Catal. **269**, 219 (2010).

[37] A. Martnez, S. Valencia, R. Murciano, H. S. Cerqueira, A. F. Costa, and E. F. S. Aguiar, Appl. Catal. A **346**, 117 (2008).

[38] A. Martnez, J. Rolln, M. A. Arribas, H. S. Cerqueira, A. F. Costa, and E. F. S. Aguiar, J. Catal. **249**, 162 (2007).